Journal of Marine Science and Technology

Volume 25 | Issue 3 Article 5

ROBUST TRAJECTORY TRACKING CONTROL OF UNDERACTUATED UNDERWATER VEHICLE SUBJECT TO UNCERTAINTIES

Yuan Chen
School of Mechanical, Electrical & Information Engineering, Shandong University at Weihai, China.

Jing Li
Yantai Industry & Trade Technician College, Yantai, China.

Kanglin Wang
School of Mechanical, Electrical & Information Engineering, Shandong University at Weihai, China.

Shurong Ning
School of Mechanical, Electrical & Information Engineering, Shandong University at Weihai, China.,
ningshurong@163.com

Recommended Citation

Chen, Yuan; Li, Jing; Wang, Kanglin; and Ning, Shurong (2017) "ROBUST TRAJECTORY TRACKING CONTROL OF UNDERACTUATED UNDERWATER VEHICLE SUBJECT TO UNCERTAINTIES," *Journal of Marine Science and Technology*: Vol. 25: Iss. 3, Article 5.
DOI: 10.6119/JMST-016-1219-1
Available at: https://jmstt.ntou.edu.tw/journal/vol25/iss3/5

ROBUST TRAJECTORY TRACKING CONTROL OF UNDERACTUATED UNDERWATER VEHICLE SUBJECT TO UNCERTAINTIES

Acknowledgements

Grateful acknowledgement is given to the financial supports from the National Natural Science Foundation of China with Grant No. 51375264 and Science and Technology Major Project of Shandong Province with Grant No. 2015JMRH0218. This work was also partially supported by State Key Laboratory of Robotics and System (HIT) with Grant No. SKLRS-2015-MS-06, and China Post-doctoral Science Foundation with Grant No. 2014T70632 and 2013M530318, and Research Awards Fund for Excellent Young and Middle-aged Scientists of Shandong Province with Grant No. BS2013ZZ008.

Journal of Marine Science and Technology, Vol. 25, No. 3, pp. 283-298 (2017)
DOI: 10.6119/JMST-016-1219-1

ROBUST TRAJECTORY TRACKING CONTROL OF UNDERACTUATED UNDERWATER VEHICLE SUBJECT TO UNCERTAINTIES

Yuan Chen[1], Jing Li[2], Kanglin Wang[1], and Shurong Ning[1]

Key words: underactuated underwater vehicle, backstepping control model, parameter uncertainties, trajectory tracking control.

ABSTRACT

A composite robust control scheme is proposed by combining a sliding mode controller with an adaptive fuzzy control algorithm to control a 3-DOF underactuated underwater vehicle with model parameter perturbations and environmental disturbances based on the backstepping control method and the Lyapunov stability theory. The adaptive fuzzy control algorithm is employed to compensate for model parameter perturbations and the sliding mode controller is adopted to eliminate the effects of environmental disturbances and approximation errors. A horizontal dynamic model and tracking error equations are established to describe the trajectory tracking control for the underactuated underwater vehicle. The relation between sliding mode control gains and model parameter uncertainties is derived to determine the error eliminating ability of the controller. The convergence and stability of the composite robust controller are demonstrated using the Lyapunov's direct method. The proposed control scheme is simulated for a 3-DOF underactuated underwater vehicle and its efficiency in the error elimination is validated in numerical simulations. Results confirm that the composite robust control law can be used to achieve a robust and preferable control performance for the horizontal trajectory tracking control of the vehicle.

I. INTRODUCTION

Many of today's underwater vehicles are underactuated vehicles due to their potential benefits over full actuated AUVs. These include a good control scheme and a streamlined shape as well as a reduction in water resistance and weight (Chen et al., 2016). Tracking and stabilization controls for underactuated underwater vehicles are difficult because of the over-possession of degrees of freedom beyond the controls (Khalid et al., 2014). Moreover, the dynamic model of an underactuated underwater vehicle is highly coupled and nonlinear due to the ever-changing nature of ocean currents and some hydrodynamic coefficients (Thor and Fossen, 2002). The underactuated underwater vehicle is so agile that the conventional linear control methods cannot fully exploit its maneuverability. Brockett's Theorem (Brockett, 1983) demonstrates that any feedback control law of a continuous time-invariant system could not stabilize the underactuated vehicle asymptotically according to the null solution.

Over the last few years, a large number of studies were conducted in the area of motion control of underactuated underwater vehicles. Control algorithms reported in the literatures can be classified into two categories: model-based control and non-model-based control. The non-model based control approach is based on the PID controller (Koh et al., 2006; Khodayari and Balochian, 2015), the neural network controller (Park, 2014) and the fuzzy controller (Raimondi and Melluso, 2010), in which each propulsive motor is controlled independently. In general, this kind of approach provides the simplest control structure but often results in poor transient performance sometimes resulting in overshoot and underdamped responses. The model-based approach, however, requires the dynamic model of underwater vehicles to define the control law and has excellent performance in quick error convergence and accuracy. The sliding model control method, a well-known model-based approach, was used to resolve the trajectory tracking control problem for underactuated underwater vehicles (Xu et al., 2015; Yan et al., 2015). However, the drag force in the model was established using a linear function of the velocity and thus was valid only at low velocities. Moreover, this kind of control method resulted in an undesired high frequency variation in the steady state. Another well-known model-based control approach is the backstepping method, which can provide a satisfactory control performance in the presence of an accurate dynamic model. Some backstepping methods were presented by some researchers (Ghommam and Saad, 2013; Li et al., 2015; Qi, 2015) for trajectory tracking control of underactuated underwater vehicles. The retainment of an accurate dynamic model, however, is a tricky task due to inevitable simplifications and other tangible factors such as backlash or friction.

Paper submitted 04/16/16; revised 09/26/16; accepted 12/19/16. Author for correspondence: Shurong Ning (e-mail: ningshurong@163.com).
[1] *School of Mechanical, Electrical & Information Engineering, Shandong University at Weihai, China.*
[2] *Yantai Industry & Trade Technician College, Yantai, China.*

Some robust backstepping controllers (Jia et al., 2012) or adaptive backstepping control approaches (Ghommam and Saad, 2013) were proposed to guarantee the control performance in presence of model parameter uncertainties. Although the effects of small parameter uncertainties on the control performances were investigated by those researchers, the relationship between the control gains and parameter uncertainties was not considered in their studies. A vehicle under the role of these controllers may lose the ability to quickly and accurately track the desired trajectories. In addition, those backstepping methods did not consider the influence of environmental disturbances and mass uncertainties in their models, which may affect their transient responses, convergence, control efforts and robustness.

In this paper, a composite robust control scheme is proposed to combine the sliding mode controller with the adaptive fuzzy control algorithm. This control scheme is used to control a 3-DOF underactuated underwater vehicle with model parameter perturbations and environmental disturbances based on backstepping control method and Lyapunov stability theory. Adaptive fuzzy control algorithm is employed to compensate for model parameter perturbation and the sliding mode controller is adopted to eliminate the effects of environmental disturbances and approximation errors. The horizontal dynamic model and tracking error equations are established for the trajectory tracking control of the underactuated underwater vehicle. The relation between the sliding mode control gains and model parameter uncertainties is derived to determine the controller's error eliminating ability. The proposed control scheme is simulated and its efficiency is tested and validated using numerical simulations of a 3-DOF underactuated underwater vehicle.

In this paper, dynamic modelling is briefly introduced in section 2 and a kinematic error model is presented in section 3. The design of the composite robust controller and its parameter selection and stability analysis are provided in sections 4 and 5, respectively. Finally, the numerical simulations and conclusions are presented in sections 6 and 7, respectively.

II. DYNAMICAL MODELING AND PROBLEM FORMULATION

The dynamic model is established in this section to describe an underactuated underwater vehicle moving in the horizontal plane. The corresponding vehicle's trajectory tracking control problem is then formulated.

1. Dynamic Modeling of an Underactuated Underwater Vehicle

The dynamic model of an underactuated underwater vehicle in the horizontal plane is first introduced. Fig. 1 illustrates an underactuated underwater vehicle and its reference frame. The inertial frame $\{O_I X_I Y_I\}$ is considered to be fixed, in which axis Z is in the gravitational direction and the other two axes (X and Y) are perpendicular to it. In contrast, the body reference frame, also known as the moving frame, is set at the geometric center of the underwater vehicle (namely, the center of gravity). The

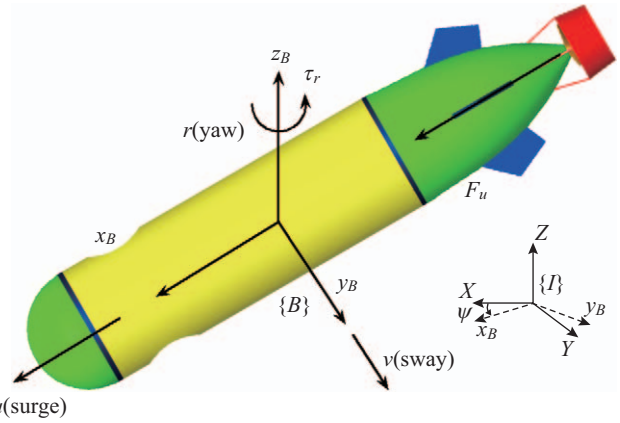

Fig. 1. The underactuated underwater vehicle and its reference frames.

longitudinal axis (x_B) points in the direction from the tail to the nose while the horizontal axis (y_B) points from the left side to the right side. According to Fossen (Thor and Fossen, 2002), the nonlinear dynamic model of the 3-DOF underactuated underwater vehicle can be written in the form of the following uniform matrix:

$$\begin{cases} \dot{\eta} = J(\psi)\upsilon \\ M\dot{\upsilon} = -C(\upsilon)\upsilon - D(\upsilon)\upsilon + w + \tau \end{cases} \tag{1}$$

where $\eta = [x, y, \psi]^T$ denotes the displacement (x, y) and the yaw angle ψ of the underwater vehicle in the inertial frame; $\upsilon = [u, v, r]^T$ represents the surge, sway, and yaw velocities of the underwater vehicle in the body reference frame while the vector $\tau = [F_u, 0, \tau_r]^T$ including the surge force of F_u and the yaw torque of τ_r. The external disturbances of the ocean current in Eq. (1) are expressed as $w = [w_1, w_2, w_3]^T$ and matrices $J(\psi)$, $D(\upsilon)$, $C(\upsilon)$, and M are defined as follows:

$$J(\psi) = \begin{bmatrix} \cos\psi & -\sin\psi & 0 \\ \sin\psi & \cos\psi & 0 \\ 0 & 0 & 1 \end{bmatrix},$$

$$D(\upsilon) = \begin{bmatrix} X_u + X_{u|u|} & 0 & 0 \\ 0 & Y_v + Y_{v|v|} & 0 \\ 0 & 0 & N_r + N_{r|r|} \end{bmatrix},$$

$$C(\upsilon) = \begin{bmatrix} 0 & 0 & -m_v v \\ 0 & 0 & m_u u \\ m_v v & -m_u u & 0 \end{bmatrix},$$

$$M = \begin{bmatrix} m_u & 0 & 0 \\ 0 & m_v & 0 \\ 0 & 0 & m_r \end{bmatrix},$$

in which $m_u = m - X_{\dot{u}}$, $m_v = m - Y_{\dot{v}}$, $m_r = I_z - N_{\dot{r}}$. In the above matrices, X_u, $X_{u|u|}$, Y_v, $Y_{v|v|}$, N_r, $N_{r|r|}$ denote the quadratic and linear drag coefficients defined in the reference (Geranmehr and Nekoo, 2015); m denotes the underwater vehicle mass and $X_{\dot{u}}$, $Y_{\dot{v}}$, $N_{\dot{r}}$ are the added masses and I_z is the inertia with respect to the vertical axis.

The nominal values of drag coefficients X_u, $X_{u|u|}$, Y_v, $Y_{v|v|}$, N_r, $N_{r|r|}$ are generally not accurate enough. The relation among the actual value Q, the nominal value Q^n, and the perturbed value Q^* of every drag coefficient can be expressed as $Q = Q^n + Q^*$. In practical applications, the perturbed value Q^* is always bounded. According to the reference (Atrp et al., 2015), the nominal value of an underwater vehicle's mass and its added mass can be easily obtained and the difference between the nominal value and the actual value is usually very small. Thus, it is assumed that the vehicle mass and the added mass satisfy the following inequality: $|m_u^*| < m_u$ and $|m_r^*| < m_r$, namely $m_u^* > \lambda m_u^n$ and $m_r^* > \lambda m_r^n$, where $-0.5 < \lambda < 0$. When the actual, the nominal, and the perturbed parameters are incorporated into the dynamic model in Eq. (1), the dynamic equation is rewritten as:

$$\begin{cases} m_u^n \dot{u} = m_v^n vr - X_u^n u - X_{u|u|}^n u|u| + \Theta_1 + w_1' + F_u \\ m_v^n \dot{v} = -m_u^n ur - Y_v^n v - Y_{v|v|}^n v|v| + \Theta_2 + w_2' \\ m_r^n \dot{r} = \left(m_u^n - m_v^n\right) uv - N_r^n r - N_{r|r|}^n r|r| + \Theta_3 + w_3' + \tau_r \end{cases} \tag{2}$$

where

$$w_1' = -m_u^* \dot{u} + m_v^* vr + w_1;\ w_2' = -m_v^* \dot{v} - m_u^* ur + w_2;$$

$$w_3' = \left(m_u^* - m_v^*\right) uv - m_r^* \dot{r} + w_3;\ \Theta_1 = -X_u^* u - X_{u|u|}^* u|u|;$$

$$\Theta_2 = -Y_v^* v - Y_{v|v|}^* v|v| \text{ and } \Theta_3 = -N_r^* r - N_{r|r|}^* r|r|.$$

2. Ocean Current Disturbances and Problem Formulation

The performance of an underwater vehicle is greatly affected by the ocean current under the ocean surface. However, this kind of disturbance is very difficult to describe accurately in the model. In order to better express the ocean current disturbances with a boundary, the disturbance $w = [w_1, w_2, w_3]^T$ is defined in the body reference frame in this paper as shown below (Thor and Fossen, 2002):

$$\dot{b}_i = \begin{cases} -T_{ii}^{-1} b_i + \Gamma_{ii} \omega_i & b_{i,\min} < b_i < b_{i,\max} \\ -T_{ii}^{-1} b_i - \Gamma_{ii} \operatorname{sgn}\left(b_i\right) |\omega_i| & b_i < b_{i,\min} \ or \ b_i > b_{i,\max} \end{cases} \tag{3}$$

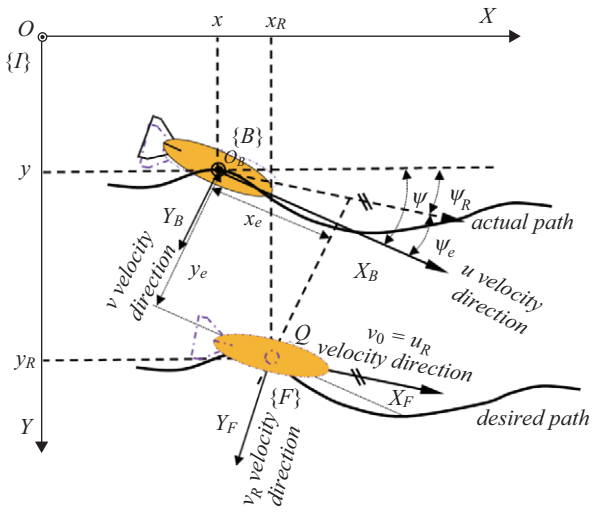

Fig. 2. The schematic diagram of horizontal path following.

$$w = \begin{cases} J^T(\psi) b & t \le 700s \\ 0 & t > 700s \end{cases} \tag{4}$$

where $w = [w_1, w_2, w_3]^T$ denotes the disturbance forces and moments in the inertial frame; $\omega \in \mathbb{R}^3$ expresses the Gauss white noise with zero mean value; $T = diag\{T_{ii}\} \in \mathbb{R}^{3\times3}$ as a positive diagonal matrix and $\Gamma = diag\{\Gamma_{ii}\} \in \mathbb{R}^{3\times3}$ as a diagonal matrix expresses Gauss white noise.

The control problem of the underactuated underwater vehicle with uncertainties can be expressed as follows: for a given desired trajectory $[x_R, y_R, \psi_R]^T$, the surge control force of F_u and the yaw control torque of τ_r should be found such that the trajectory tracking error vector $[x_e, y_e, \psi_e]^T = [x_R - x, y_R - y, \psi_R - \psi]^T$, where the vector $[x, y, \psi]^T$ denotes the actual trajectory, converges to a value near the original point with a very small oscillation.

III. KINEMATIC ERROR MODEL OF AN UNDERACTUATED UNDERWATER VEHICLE

In this section, a kinematic error model is established to describe the trajectory tracking control for the underactuated underwater vehicle and is used to guide the design of controllers. In Fig. 2, $\{O_B X_B Y_B\}$, $\{OXY\}$ and $\{O_F X_F Y_F\}$ represent the actual body-fixed frame, the inertial frame and the desired path constitute frame respectively, where Q is an arbitrary point on the desired tracking path to be followed. The coordinates of virtual point Q on the desired tracking path of $Q_R = [x_R, y_R, \psi_R]^T$ can be described as a function of time and thus the position of point Q in the inertial frame on the actual path can be expressed as:

$$Q = \left[x, y, \psi\right]^T \tag{5}$$

The desired horizontal velocity v_R of the underwater vehicle is far smaller than its desired longitudinal velocity u_R when no extremely large external disturbances exist. Moreover, the influence of the horizontal velocity on the tracking performance is also not significant. In order to ensure the smoothness of tracking curves, x_R and y_R are required to be continuously differentiable. Thus, the desired velocity at virtual point Q in the inertial frame can be defined as:

$$v_Q = u_R = \sqrt{\dot{x}_R{}^2 + \dot{y}_R{}^2} \tag{6}$$

The intersection angle of ψ_R between the desired velocity vector of v_Q and the horizontal axis in the inertial frame is defined as the rotational angle from frame $\{O_B X_B Y_B\}$ to frame $\{OXY\}$ and can be expressed as:

$$\psi_R = \begin{cases} \arctan\left(\dfrac{\dot{y}_R}{\dot{x}_R}\right) & \dot{x}_R \geq 0 \\ \pi + \arctan\left(\dfrac{\dot{y}_R}{\dot{x}_R}\right) & \dot{x}_R < 0 \end{cases} \tag{7}$$

By defining $Q = [x, y, \psi]^T$ as the actual position vector of the underwater vehicle in the inertial frame and $Q_R = [x_R, y_R, \psi_R]^T$ as the desired position vector of the point, the tracking error vector, $\varepsilon = [x_e, y_e, \psi_e]^T$, can be expressed in the actual body-fixed frame by the following equation:

$$\varepsilon = R(\psi)(Q_R - Q) \tag{8}$$

where $R(\psi)$ is the rotation transformation matrix from the inertial frame to the body-fixed frame and is parameterized locally by angle ψ with the following relationship:

$$R(\psi) = \begin{bmatrix} \cos\psi & \sin\psi & 0 \\ -\sin\psi & \cos\psi & 0 \\ 0 & 0 & 1 \end{bmatrix} \tag{9}$$

By taking the derivative of ε, Eq. (8) becomes

$$\dot{\varepsilon} = \dot{R}(\psi)(Q_R - Q) + R(\psi)\left(\dot{Q}_R - \dot{Q}\right) \tag{10}$$

where $\dot{R}(\psi) = R(\psi)S(\dot{\psi}) = S(\dot{\psi})R(\psi)$ and

$$S(\dot{\psi}) = \begin{bmatrix} 0 & \dot{\psi} & 0 \\ -\dot{\psi} & 0 & 0 \\ 0 & 0 & 1 \end{bmatrix}.$$

Eq. (10) can be rewritten as

$$\begin{aligned} \dot{\varepsilon} &= S(\dot{\psi})R(\psi)(Q_R - Q) + R(\psi)\left(\dot{Q}_R - \dot{Q}\right) \\ &= S(\dot{\psi})\varepsilon + R(\psi)\left(\dot{Q}_R - R^T(\psi)\begin{bmatrix} u \\ v \\ r \end{bmatrix}\right) \\ &= S(\dot{\psi})\varepsilon + \begin{bmatrix} \dot{x}_R\cos\psi + \dot{y}_R\sin\psi \\ -\dot{x}_R\sin\psi + \dot{y}_R\cos\psi \\ \dot{\psi}_R \end{bmatrix} - \begin{bmatrix} u \\ v \\ r \end{bmatrix} \end{aligned} \tag{11}$$

Symbol ψ_e in Fig. 2 denotes the intersection angle between the desired velocity v_Q and the longitudinal axis in the actual body-fixed frame and can be calculated from the difference between the actual yaw angle (ψ) and the desired yaw angle (ψ_R) as $\psi_e = \psi - \psi_R$. The second term of $\left[\dot{x}_R\cos\psi + \dot{y}_R\sin\psi, -\dot{x}_R\sin\psi + \dot{y}_R\cos\psi, \dot{\psi}_R\right]^T$ in Eq. (11) represents the velocity components in the actual body-fixed frame for the desired velocity vector $\left[\dot{x}_R, \dot{y}_R, \dot{\psi}_R\right]^T$ in the inertial frame. When two velocity components $\dot{x}_R$ and $\dot{y}_R$ are synthesized into the desired velocity v_Q as defined by $v_Q = \sqrt{\dot{x}_R{}^2 + \dot{y}_R{}^2}$, the two terms $\dot{x}_R\cos\psi + \dot{y}_R\sin\psi$ and $-\dot{x}_R\sin\psi + \dot{y}_R\cos\psi$ in Eq. (11) can be thus expressed as $v_Q\cos\psi_e$ and $v_Q\sin\psi_e$ respectively. With a few manipulations, Eq. (11) becomes

$$\begin{aligned} \dot{\varepsilon} &= \begin{bmatrix} 0 & \dot{\psi} & 0 \\ -\dot{\psi} & 0 & 0 \\ 0 & 0 & 1 \end{bmatrix}\begin{bmatrix} x_e \\ y_e \\ \psi_e \end{bmatrix} + \begin{bmatrix} v_Q\cos\psi_e \\ v_Q\sin\psi_e \\ \dot{\psi}_R \end{bmatrix} - \begin{bmatrix} u \\ v \\ r \end{bmatrix} \\ &= \begin{bmatrix} ry_e + v_Q\cos\psi_e - u \\ -rx_e + v_Q\sin\psi_e - v \\ -r + \dot{\psi}_R + \psi_e \end{bmatrix} \end{aligned} \tag{12}$$

IV. CONTROLLER DESIGN

In this section, surge force F_u and yaw moment τ_r are derived according to the backstepping control method and Lyapunov theory. Based on the error model in Eq. (12) in the body-fixed frame, a nonlinear backstepping method is adopted to design the controller following a desired path. The controller design process is outlined in the following steps:

Step 1: Define the Lyapunov function as $V_1 = \frac{1}{2}\left(x_e^2 + y_e^2\right)$ and take the time derivative of V_1. Substituting the first two terms in the error model of Eq. (12) into the time derivative equation of V_1 results in the following time derivative of V_1:

$$\dot{V}_1 = x_e\left(v_Q\cos\psi_e - u\right) + y_e\left(v_Q\sin\psi_e - v\right) \tag{13}$$

Now, let us introduce two virtual control functions u and v with their desired values u_r and v_r designed as $u_r = k_x x_e + v_Q \cos\psi_e$ and $v_r = k_y y_e + v_Q \sin\psi_e$, where k_x and k_y are two positive constants. Substituting the two desired values of u_r and v_r into Eq. (13) yields $\dot{V}_1 = -k_x x_e^2 - k_y y_e^2$. Since u_r and v_r are not the actual control functions of the underwater vehicle, the two error variables u_e and v_e can be expressed as $u_e = u - u_r$ and $v_e = v - v_r$. Consequently, the time derivative equation of V_1 becomes

$$\dot{V}_1 = -k_x x_e^2 - k_y y_e^2 - u_e x_e - v_e y_e \tag{14}$$

Step 2: For the consideration of the stabilization of the error variable u_e and v_e, the following Lyapunov function is used:

$$V_2 = V_1 + \frac{1}{2}u_e^2 + \frac{1}{2}v_e^2 \tag{15}$$

The time derivative of V_2 becomes

$$\dot{V}_2 = -k_x x_e^2 - k_y y_e^2 - v_e\left(y_e - \dot{v} + \dot{v}_r\right) + u_e\left(\dot{u} - \dot{u}_r - x_e\right) \tag{16}$$

The actual control force F_u is then obtained as follows:

$$\begin{aligned} F_u = {} & X_u^n u + X_{u|u|}^n u|u| - m_v^n vr - \rho_1 \operatorname{sgn}(u_e) \\ & + m_u^n\left(\dot{u}_r + x_e - k_u u_e\right) + \hat{\Theta}_1 \end{aligned} \tag{17}$$

where k_u and ρ_1 are two positive constants and u_r is the desired surge acceleration along the longitudinal direction. The following adaptive fuzzy control signal $\hat{\Theta}_1$ and its adaptive control law are designed to eliminate the uncertainty $-X_u^* u - X_{u|u|}^* u|u|$ of Θ_1 in Eq. (2).

$$\hat{\Theta}_1 = -\hat{\eta}_1^T \varphi(e_s) \tanh\left(\frac{\hat{\eta}_1^T \varphi(e_s)}{\varepsilon}\right) \tag{18}$$

$$\dot{\hat{\eta}}_1^T = \lambda_1 u_e \varphi^T(e_s) \tag{19}$$

where $e_s = [u_e, v_e, r_e]^T$ consists of the velocity error vector of the surge, sway, and yaw velocities in the body reference frame; $\varphi(e_s)$ represents the adaptive fuzzy base function; $\hat{\eta}_1^T$ is the adaptive control parameter; $\lambda_1 \in R$ is a positive constant and ε is an arbitrary small positive constant.

Let $\eta_1^T \varphi(e_s) \tanh\left(\frac{\eta_1^T \varphi(e_s)}{\varepsilon}\right)$ be a close approximation of $-X_u^* u - X_{u|u|}^* u|u|$ of Θ_1 in Eq. (2). Substituting Eq. (17) into the first term of Eq. (2) yields

$$\dot{u} - \dot{u}_r - x_e = -k_u u_e + \left(m_u^n\right)^{-1} \begin{pmatrix} \left(w_1' - \rho_1 \operatorname{sgn}(u_e)\right) - \hat{\eta}_1^T \varphi(e_s) \tanh\left(\frac{\hat{\eta}_1^T \varphi(e_s)}{\varepsilon}\right) \\ + \eta_1^T \varphi(e_s) \tanh\left(\frac{\eta_1^T \varphi(e_s)}{\varepsilon}\right) \end{pmatrix}.$$

Then, Eq. (16) can be rewritten as

$$\begin{aligned} \dot{V}_2 = {} & -k_x x_e^2 - k_y y_e^2 - v_e\left(y_e - \dot{v} + \dot{v}_r\right) - k_u u_e^2 \\ & + \left(m_u^n\right)^{-1} u_e\left(w_1' - \rho_1 \operatorname{sgn}(u_e)\right) \\ & - \left(m_u^n\right)^{-1} u_e \hat{\eta}_1^T \varphi(e_s) \tanh\left(\frac{\hat{\eta}_1^T \varphi(e_s)}{\varepsilon}\right) \\ & + \left(m_u^n\right)^{-1} u_e \eta_1^T \varphi(e_s) \tanh\left(\frac{\eta_1^T \varphi(e_s)}{\varepsilon}\right) \end{aligned} \tag{20}$$

where

$$\begin{aligned} w_1' = {} & m_u^{-1}\left(m_u^* \rho_1 \operatorname{sgn}(u_e)\right. \\ & \left. + m_u^n\left(-m_u^*\left(\dot{u}_r + x_e - k_u u_e\right) + m_v^* vr + w_1\right)\right) \end{aligned} \tag{21}$$

Step 3: To stabilize the error variables ψ_e and $\tilde{\eta}_1$, the following Lyapunov function is employed:

$$V_3 = V_2 + \frac{1}{2}\psi_e^2 + \frac{1}{2}\lambda_1^{-1}\left(m_u^n\right)^{-1} \tilde{\eta}_1^T \tilde{\eta}_1 \tag{22}$$

and its corresponding time derivative is then expressed as

$$\begin{aligned} \dot{V}_3 = {} & -k_x x_e^2 - k_y y_e^2 - v_e\left(y_e - \dot{v} + \dot{v}_r\right) \\ & - k_u u_e^2 + \left(m_u^n\right)^{-1} u_e\left(w_1' - \rho_1 \operatorname{sgn}(u_e)\right) + \psi_e \dot{\psi}_e \\ & - \left(m_u^n\right)^{-1} u_e \hat{\eta}_1^T \varphi(e_s) \tanh\left(\frac{\hat{\eta}_1^T \varphi(e_s)}{\varepsilon}\right) \\ & + \left(m_u^n\right)^{-1} u_e \eta_1^T \varphi(e_s) \tanh\left(\frac{\eta_1^T \varphi(e_s)}{\varepsilon}\right) \\ & + \lambda_1^{-1}\left(m_u^n\right)^{-1} \dot{\tilde{\eta}}_1^T \tilde{\eta}_1 \end{aligned} \tag{23}$$

To eliminate the uncertainty of $-Y_v^* v - Y_{v|v|}^* v|v|$ or Θ_2 in Eq. (2), the adaptive fuzzy control signal $\hat{\Theta}_2$ and its adaptive control law are adopted and expressed as $\hat{\Theta}_2 = -\hat{\eta}_2^T \varphi(e_s) \tanh\left(\frac{\hat{\eta}_2^T \varphi(e_s)}{\varepsilon}\right)$ and $\dot{\hat{\eta}}_2^T = \lambda_2 v_e \varphi^T(e_s)$, in which $\hat{\eta}_2^T$ is the adaptive control parameter; $\varphi(e_s)$ is the adaptive fuzzy base function; $\lambda_2 \in R$ is a positive constant and ε is an arbitrary small positive constant. Substituting the adaptive fuzzy control signal of Θ_2 and $w_2' = -m_v^* \dot{v} - m_u^* ur + w_2$ into the second term of Eq. (2) with a few manipulations yields

$$\dot{v} = -m_v^{-1}\left(m_u ur + w_2 - Y_v v - Y_{v|v|} v|v|\right) + \left(m_v^n\right)^{-1} \begin{pmatrix} -\hat{\eta}_2^T \varphi(e_s) \tanh\left(\frac{\hat{\eta}_2^T \varphi(e_s)}{\varepsilon}\right) \\ +\eta_2^T \varphi(e_s) \tanh\left(\frac{\eta_2^T \varphi(e_s)}{\varepsilon}\right) \end{pmatrix}.$$

The virtual control r_r can be expressed in the form of $r_r = \dot{\psi}_R + k_\psi \psi_e$. Therefore, Eq. (23) can be re-written using the above expressions for $\dot{v}$ and r_r with $\dot{\psi}_e = \dot{\psi}_R - r$

$$\begin{aligned} \dot{V}_3 = & -k_x x_e^2 - k_y y_e^2 - k_u u_e^2 - k_\psi \psi_e^2 - k_\psi \psi_e m_v^{-1} m_u u v_e \\ & + \left(m_u^n\right)^{-1} u_e \left(w_1' - \rho_1 \operatorname{sgn}(u_e)\right) \\ & - \left(m_u^n\right)^{-1} u_e \hat{\eta}_1^T \varphi(e_s) \tanh\left(\frac{\hat{\eta}_1^T \varphi(e_s)}{\varepsilon}\right) \\ & + \lambda_1^{-1} \left(m_u^n\right)^{-1} \dot{\hat{\eta}}_1^T \tilde{\eta}_1 + \sigma \\ & + \left(m_u^n\right)^{-1} u_e \eta_1^T \varphi(e_s) \tanh\left(\frac{\eta_1^T \varphi(e_s)}{\varepsilon}\right) \\ & - \left(m_v^n\right)^{-1} v_e \hat{\eta}_2^T \varphi(e_s) \tanh\left(\frac{\hat{\eta}_2^T \varphi(e_s)}{\varepsilon}\right) \\ & + \left(m_v^n\right)^{-1} v_e \eta_2^T \varphi(e_s) \tanh\left(\frac{\eta_2^T \varphi(e_s)}{\varepsilon}\right) \end{aligned} \tag{24}$$

where

$$\sigma = -v_e m_v^{-1}\left(m_v y_e + Y_v v + Y_{v|v|} v|v| + m_v \dot{v}_r - w_2 + m_u u \dot{\psi}_R\right).$$

Because variable r_r is not an actual control parameter, it can be replaced with an error expression of $r_e = r - r_r$. Then, substituting the adaptive control law of $\dot{\tilde{\eta}}_1^T = \dot{\hat{\eta}}_1^T$ in Eq. (19) into Eq. (24) yields

$$\begin{aligned} \dot{V}_3 = & -k_x x_e^2 - k_y y_e^2 - k_u u_e^2 - k_\psi \psi_e^2 - k_\psi \psi_e m_v^{-1} m_u u v_e \\ & + \left(m_u^n\right)^{-1} u_e \left(w_1' - \rho_1 \operatorname{sgn}(u_e)\right) \\ & - \left(\psi_e + m_v^{-1} m_u u v_e\right) r_e + \sigma \\ & - \left(m_u^n\right)^{-1} u_e \hat{\eta}_1^T \varphi(e_s) \tanh\left(\frac{\hat{\eta}_1^T \varphi(e_s)}{\varepsilon}\right) \\ & + \left(m_u^n\right)^{-1} u_e \tilde{\eta}_1^T \varphi(e_s) \\ & + \left(m_u^n\right)^{-1} u_e \eta_1^T \varphi(e_s) \tanh\left(\frac{\eta_1^T \varphi(e_s)}{\varepsilon}\right) \\ & - \left(m_v^n\right)^{-1} v_e \hat{\eta}_2^T \varphi(e_s) \tanh\left(\frac{\hat{\eta}_2^T \varphi(e_s)}{\varepsilon}\right) \\ & + \left(m_v^n\right)^{-1} v_e \eta_2^T \varphi(e_s) \tanh\left(\frac{\eta_2^T \varphi(e_s)}{\varepsilon}\right) \end{aligned} \tag{25}$$

Step 4: In this step, a controller for error vectors r_e and $\tilde{\eta}_2$ stabilization is introduced using the following Lyapunov function:

$$V_4 = V_3 + \frac{1}{2} r_e^2 + \frac{1}{2} \lambda_2^{-1} \left(m_v^n\right)^{-1} \tilde{\eta}_2^T \tilde{\eta}_2 \tag{26}$$

By taking the time derivative of V_4 and substituting the term of $\dot{r}_e = \dot{r} - \dot{r}_r$ and the adaptive control law of $\dot{\tilde{\eta}}_2^T = \dot{\hat{\eta}}_2^T$ into the time derivative of V_4, the time derivative of V_4 can be expressed as

$$\begin{aligned} \dot{V}_4 = & -k_x x_e^2 - k_y y_e^2 - k_u u_e^2 - k_\psi \psi_e^2 + \left(\dot{r} - \dot{r}_r - m_v^{-1} m_u u v_e - \psi_e\right) r_e \\ & - k_\psi \psi_e m_v^{-1} m_u u v_e + \left(m_u^n\right)^{-1} u_e \left(w_1' - \rho_1 \operatorname{sgn}(u_e)\right)_e + \sigma \\ & - \left(m_u^n\right)^{-1} u_e \hat{\eta}_1^T \varphi(e_s) \tanh\left(\frac{\hat{\eta}_1^T \varphi(e_s)}{\varepsilon}\right) + \left(m_u^n\right)^{-1} u_e \tilde{\eta}_1^T \varphi(e_s) \\ & + \left(m_u^n\right)^{-1} u_e \eta_1^T \varphi(e_s) \tanh\left(\frac{\eta_1^T \varphi(e_s)}{\varepsilon}\right) + \left(m_v^n\right)^{-1} v_e \tilde{\eta}_2^T \varphi(e_s) \\ & - \left(m_v^n\right)^{-1} v_e \hat{\eta}_2^T \varphi(e_s) \tanh\left(\frac{\hat{\eta}_2^T \varphi(e_s)}{\varepsilon}\right) \\ & + \left(m_v^n\right)^{-1} v_e \eta_2^T \varphi(e_s) \tanh\left(\frac{\eta_2^T \varphi(e_s)}{\varepsilon}\right) \end{aligned} \tag{27}$$

The actual control law of the yaw torque of τ_r is obtained as follows:

$$\tau_r = N_r^n r + N_{r|r|}^n r|r| - \left(m_u^n - m_v^n\right)uv - \rho_3 \operatorname{sgn}\left(r_e\right) + m_r^n\left(\dot{r}_r + \psi_e - k_r r_e\right) + \hat{\Theta}_3 \tag{28}$$

To eliminate the uncertainty of $-N_r^* r - N_{r|r|}^* r|r|$ or Θ_3 in Eq. (2), the adaptive fuzzy control signal $\hat{\Theta}_3$ in Eq. (28) and its adaptive control law are defined as $\hat{\Theta}_3 = -\hat{\eta}_3^T \varphi\left(e_s\right)\tanh\left(\frac{\hat{\eta}_3^T \varphi\left(e_s\right)}{\varepsilon}\right)$ and $\dot{\hat{\eta}}_3^T = \lambda_3 v_e \varphi^T\left(e_s\right)$, in which $\hat{\eta}_3^T$ is the adaptive control parameter; $\varphi(e_s)$ is the adaptive fuzzy base function; $\lambda_3 \in R$ is a positive constant and ε is an arbitrary small positive constant. Substituting τ_r in Eq. (28) into the third term of Eq. (2) with a few manipulations results in

$$\dot{r} - \dot{r}_r = \left(m_r^n\right)^{-1}\begin{pmatrix} w_3 + m_r^n \psi_e - m_r^n k_r r_e - \rho_3 \operatorname{sgn}\left(r_e\right) \\ -\hat{\eta}_3^T \varphi\left(e_s\right)\tanh\left(\frac{\hat{\eta}_3^T \varphi\left(e_s\right)}{\varepsilon}\right) + \eta_3^T \varphi\left(e_s\right)\tanh\left(\frac{\eta_3^T \varphi\left(e_s\right)}{\varepsilon}\right) \end{pmatrix}.$$

Then, Eq. (27) becomes

$$\begin{aligned}\dot{V}_4 = & -k_x x_e^2 - k_y y_e^2 - k_u u_e^2 - k_\psi \psi_e^2 - k_\psi \psi_e m_v^{-1} m_u u v_e \\ & + \left(m_u^n\right)^{-1} u_e\left(w_1' - \rho_1 \operatorname{sgn}\left(u_e\right)\right) + \left(m_r^n\right)^{-1} r_e\left(w_3' - \rho_3 \operatorname{sgn}\left(r_e\right)\right) \\ & + \sigma - k_r r_e^2 - m_v^{-1} m_u u v_e\left(r - \dot{\psi}_R\right) - \left(m_u^n\right)^{-1} u_e \hat{\eta}_1^T \varphi\left(e_s\right)\tanh\left(\frac{\hat{\eta}_1^T \varphi\left(e_s\right)}{\varepsilon}\right) \\ & + \left(m_u^n\right)^{-1} u_e \tilde{\eta}_1^T \varphi\left(e_s\right) + \left(m_u^n\right)^{-1} u_e \eta_1^T \varphi\left(e_s\right)\tanh\left(\frac{\eta_1^T \varphi\left(e_s\right)}{\varepsilon}\right) \\ & + \left(m_v^n\right)^{-1} v_e \tilde{\eta}_2^T \varphi\left(e_s\right) - \left(m_v^n\right)^{-1} v_e \hat{\eta}_2^T \varphi\left(e_s\right)\tanh\left(\frac{\hat{\eta}_2^T \varphi\left(e_s\right)}{\varepsilon}\right) \\ & + \left(m_v^n\right)^{-1} v_e \eta_2^T \varphi\left(e_s\right)\tanh\left(\frac{\eta_2^T \varphi\left(e_s\right)}{\varepsilon}\right) - \left(m_r^n\right)^{-1} r_e \hat{\eta}_3^T \varphi\left(e_s\right)\tanh\left(\frac{\hat{\eta}_3^T \varphi\left(e_s\right)}{\varepsilon}\right) \\ & + \left(m_r^n\right)^{-1} r_e \eta_3^T \varphi\left(e_s\right)\tanh\left(\frac{\eta_3^T \varphi\left(e_s\right)}{\varepsilon}\right)\end{aligned} \tag{29}$$

where

$$w_3' = m_r^n m_r^{-1}\begin{pmatrix} \left(m_u^* - m_v^*\right)uv \\ -m_r^*\left(\dot{r}_r - m_u^n\left(m_v^n\right)^{-1} u v_e + \psi_e - k_r r_e\right) + w_3 \end{pmatrix} + m_r^* m_r^{-1}\rho_3 \operatorname{sgn}\left(r_e\right) \tag{30}$$

Step 5: To stabilize the error variables of $\tilde{\eta}_3$, the following Lyapunov function is selected:

$$V_5 = V_4 + \frac{1}{2}\lambda_3^{-1}\left(m_r^n\right)^{-1}\tilde{\eta}_3^T \tilde{\eta}_3 \tag{31}$$

The corresponding time derivative of V_5 becomes by substituting the adaptive control law of $\dot{\tilde{\eta}}_3^T = \dot{\hat{\eta}}_3^T = \lambda_3 r_e \varphi^T\left(e_s\right)$ into Eq. (31):

$$\begin{aligned}\dot{V}_5 = & -k_x x_e^2 - k_y y_e^2 - k_u u_e^2 - k_\psi \psi_e^2 - k_\psi \psi_e m_v^{-1} m_u u v_e \\ & + \left(m_u^n\right)^{-1} u_e\left(w_1' - \rho_1 \operatorname{sgn}\left(u_e\right)\right) + \left(m_r^n\right)^{-1} r_e\left(w_3' - \rho_3 \operatorname{sgn}\left(r_e\right)\right) \\ & + \sigma - k_r r_e^2 - m_v^{-1} m_u u v_e\left(r - \dot{\psi}_R\right) \\ & - \left(m_u^n\right)^{-1} u_e \hat{\eta}_1^T \varphi\left(e_s\right)\tanh\left(\frac{\hat{\eta}_1^T \varphi\left(e_s\right)}{\varepsilon}\right) + \left(m_u^n\right)^{-1} u_e \tilde{\eta}_1^T \varphi\left(e_s\right) \\ & + \left(m_u^n\right)^{-1} u_e \eta_1^T \varphi\left(e_s\right)\tanh\left(\frac{\eta_1^T \varphi\left(e_s\right)}{\varepsilon}\right) + \left(m_v^n\right)^{-1} v_e \tilde{\eta}_2^T \varphi\left(e_s\right) \\ & - \left(m_v^n\right)^{-1} v_e \hat{\eta}_2^T \varphi\left(e_s\right)\tanh\left(\frac{\hat{\eta}_2^T \varphi\left(e_s\right)}{\varepsilon}\right) + \left(m_v^n\right)^{-1} v_e \eta_2^T \varphi\left(e_s\right)\tanh\left(\frac{\eta_2^T \varphi\left(e_s\right)}{\varepsilon}\right) \\ & - \left(m_r^n\right)^{-1} r_e \hat{\eta}_3^T \varphi\left(e_s\right)\tanh\left(\frac{\hat{\eta}_3^T \varphi\left(e_s\right)}{\varepsilon}\right) + \left(m_r^n\right)^{-1} r_e \eta_3^T \varphi\left(e_s\right)\tanh\left(\frac{\eta_3^T \varphi\left(e_s\right)}{\varepsilon}\right) \\ & + \left(m_r^n\right)^{-1} r_e\left(\tilde{\eta}_3^T \varphi\left(e_s\right)\right)^T\end{aligned} \tag{32}$$

V. CONTROL PARAMETER SELECTION AND STABILITY ANALYSIS

The relation between sliding mode control gains and model parameter uncertainties is obtained in this section to assess the error eliminating ability of the controller. In the meantime, the asymptotic stability of the overall system is also demonstrated based on Lyapunov stability theory.

First, the following Lemma is introduced on a bounded property:

Lemma 1. The following inequality holds for any $\varepsilon > 0$ and any $\zeta \in R$ (Polycarpou and Ioannou, 1996):

$$0 \le |\zeta| - \zeta\tanh\left(\frac{\zeta}{\varepsilon}\right) \le \kappa\varepsilon \tag{33}$$

where κ is a positive constant that satisfies $\kappa = e^{-(\kappa+1)}$, i.e., $\kappa = 0.2785$.

The two robust control terms of $\rho_1\, sgn\,(u_e)$ in the control force of F_u in Eq. (17) and $\rho_3\, sgn\,(r_e)$ in the yaw control torque of τ_r in Eq. (28) are used to eliminate the two uncertainties of w_1' and w_3' in Eqs. (21) and (30) respectively. The two positive constants of ρ_1 and ρ_3 in the two robust control terms directly determine the error eliminating ability for the controller. The two uncertainties in Eqs. (21) and (30) can be rewritten as

$$w_1' = m_u^{-1} m_u^* \rho_1 \operatorname{sgn}\left(u_e\right) + m_u^{-1} m_u^n \varepsilon_u \tag{34}$$

$$w_3' = m_r^{-1} m_r^* \rho_3 \operatorname{sgn}\left(r_e\right) + m_r^{-1} m_r^n \varepsilon_r \tag{35}$$

where

$$\varepsilon_u = m_v^* vr + w_1 - m_u^* \left(\dot{u}_r + x_e - k_u u_e\right) \text{ and}$$

$$\varepsilon_r = \left(m_u^* - m_v^*\right)uv + w_3 - m_r^* \left(\dot{r}_r + \psi_e - \left(m_v^n\right)^{-1} m_u^n uv_e - k_r r_e\right).$$

It is known that $|a+b| \le |a| + |b|$ when a and b are two real numbers, Thus, taking the absolute value on both sides of the equation for Eqs. (34) and (35) results in the following two inequalities

$$\left|w_1^{'}\right| \le m_u^{-1}\left|m_u^*\right|\rho_1 + m_u^{-1} m_u^n \left|\varepsilon_u\right| \tag{36}$$

$$\left|w_3^{'}\right| \le m_r^{-1}\left|m_r^*\right|\rho_3 + m_r^{-1} m_r^n \left|\varepsilon_r\right| \tag{37}$$

It can be seen from inequality (36) that when $\left|m_u^*\right| \ge m_u$, the uncertainty cannot be guaranteed to be eliminated by the surge control force of F_u. Similarly, as seen from Eq. (37), when $\left|m_r^*\right| \ge m_r$, the uncertainty cannot be guaranteed to be eliminated by the yaw control torque of τ_r. In other words, the uncertainties of $w_1^{'}$ and $w_3^{'}$ may be greater than the two robust positive constants of ρ_1 and ρ_3. Thus, the two uncertainty masses of $\left|m_u^*\right|$ and $\left|m_r^*\right|$ must be assumed to satisfy $\left|m_u^*\right| < m_u$ and $\left|m_r^*\right| < m_r$, namely $m_u^* > \lambda m_u^n$ and $m_r^* > \lambda m_r^n$ for -0.5 < λ <0. Let $\rho_1 \ge \max\left(\left(m_u - \left|m_u^*\right|\right)^{-1} m_u^n \left|\varepsilon_u\right|\right)$ and $\rho_3 \ge \max\left(\left(m_r - \left|m_r^*\right|\right)^{-1} m_r^n \left|\varepsilon_r\right|\right)$. The following inequalities hold true:

$$\left|\varepsilon_u\right| \le \left(m_u^n\right)^{-1}\left(m_u - \left|m_u^*\right|\right)\rho_1 \tag{38}$$

$$\left|\varepsilon_r\right| \le \left(m_r^n\right)^{-1}\left(m_r - \left|m_r^*\right|\right)\rho_3 \tag{39}$$

Substituting inequalities (38) and (39) into inequalities (36) and (37) respectively yields $\left|w_1^{'}\right| \le \rho_1$ and $\left|w_3^{'}\right| \le \rho_3$. Thus, the uncertainties can be eliminated by the surge control force of F_u and the yaw control torque of τ_r if the mass and robust control parameters satisfy conditions of

1. $\left|m_u^*\right| < m_u$ and $\left|m_r^*\right| < m_r$;
2. $\rho_1 \ge \max\left(\left(m_u - \left|m_u^*\right|\right)^{-1} m_u^n \left|\varepsilon_u\right|\right)$ and $\rho_3 \ge \max\left(\left(m_r - \left|m_r^*\right|\right)^{-1} m_r^n \left|\varepsilon_r\right|\right)$.

When $m_u^* \ge 0$ and $m_r^* \ge 0$, $m_u^n \big/ \left(m_u - \left|m_u^*\right|\right) = 1$ and $m_r^n \big/ \left(m_r - \left|m_r^*\right|\right) = 1$. When $m_u^* < 0$ and $m_r^* < 0$, the maximum value of both $m_u^n \big/ \left(m_u - \left|m_u^*\right|\right)$ and $m_r^n \big/ \left(m_r - \left|m_r^*\right|\right)$ is equal to $1/(1+2\lambda)$. Thus, the boundary conditions for ρ_1 and ρ_3 become ρ_1 or $\rho_3 \ge \max\left(\left|\varepsilon_u\right|\right)/(1+2\lambda)$. For a given value of $\max\left(\left|\varepsilon_u\right|\right)$ and uncertainty value of $\left|m^*\right|$, the following conditions must hold: the control parameters of ρ_1 and ρ_3 need to satisfy the following inequality ρ_1 or $\rho_3 \ge \max\left(\left|\varepsilon_u\right|\right)$ when m_u^* and m_r^* are positive values and to meet the boundary conditions of ρ_1 or $\rho_3 \ge \max\left(\left|\varepsilon_u\right|\right)/(1+2\lambda)$ when m_u^* and m_r^* are negative values. The boundary values for negative values of m_u^* and m_r^* are larger than that for positive values of m_u^* and m_r^*. In other words, the control cost for $m_u^* < 0$ and $m_r^* < 0$ is more than that for positive values of m_u^* and m_r^*.

Since $\left\|\tanh\left(\frac{\hat{\eta}_i^T \varphi(e_s)}{\varepsilon}\right)\right\| \le 1$, thus $\hat{\eta}_i^T \varphi(e_s) + \eta_i^T \varphi(e_s) \tanh\left(\frac{\eta_i^T \varphi(e_s)}{\varepsilon}\right) \le \hat{\eta}_i^T \varphi(e_s)$. Let $\zeta_1 = \hat{\eta}_1^T \varphi(e_s)$, $\zeta_2 = \hat{\eta}_2^T \varphi(e_s)$ and $\zeta_3 = \hat{\eta}_3^T \varphi(e_s)$. Then the following inequalities can be obtained based on Lemma 1: $|\zeta_i| - \zeta_i \tanh\left(\frac{\zeta_i}{\varepsilon}\right) \le \kappa_i \varepsilon$. Additionally, by using the two inequalities $\left(m_u^n\right)^{-1} u_e\left(w_1^{'} - \rho_1 \operatorname{sgn}(u_e)\right) \le 0$ and $\left(m_r^n\right)^{-1} r_e\left(w_3^{'} - \rho_3 \operatorname{sgn}(r_e)\right) \le 0$, Eq. (32) can be rewritten as:

$$\begin{aligned} \dot{V}_5 \le & -k_x x_e^2 - k_y y_e^2 - k_u u_e^2 - k_\psi \psi_e^2 - k_\psi \psi_e m_v^{-1} m_u uv_e \\ & - k_r r_e^2 + \sigma - m_v^{-1} m_u uv_e \left(r - \dot{\psi}_R\right) \end{aligned} \tag{40}$$

Taking the time derivative of $v_r = k_y y_e + v_Q \sin\psi_e$ and then substituting the second term of Eq. (12) into the derivative equation yields

$$\begin{aligned} \dot{v}_r = & \dot{v}_Q \sin\psi_e + v_Q\left(\dot{\psi}_R - r\right)\cos\psi_e \\ & + k_y\left(-v + v_Q \sin\psi_e - r x_e\right) \end{aligned} \tag{41}$$

Substituting Eq. (41) into σ in Eq. (24) gets

$$\sigma = -v_e m_v^{-1} \begin{pmatrix} m_v y_e + Y_v v + Y_{v|v|} v|v| + m_v \begin{pmatrix} \dot{v}_Q \sin\psi_e + v_Q\left(\dot{\psi}_R - r\right)\cos\psi_e \\ + k_y\left(-v + v_Q \sin\psi_e - r x_e\right) \end{pmatrix} \\ -w_2 + m_u u \dot{\psi}_R \end{pmatrix} \tag{42}$$

And then substituting Eq. (42) into Eq. (40) yields

$$\dot{V}_5 \le k_y |r|_{\max} v_e x_e + \left(|\dot{v}_Q|_{\max} + |k_\psi v_Q|_{\max} + |k_\psi m_v^{-1} m_u u|_{\max}\right)|v_e \psi_e| - v_e y_e - k_x x_e^2 - k_y y_e^2 - k_u u_e^2 - k_\psi \psi_e^2 - k_\psi \psi_e m_v^{-1} m_u u v_e - k_r r_e^2 + |v_e|\zeta \quad (43)$$

where the subscript "max" denotes the maximum value and the value of η can be expressed $\zeta = m_v^{-1}\left(m_v |v_Q(\dot{\psi}_R - r)|_{\max} + m_u |ur|_{\max} + (Y_v + m_v k_y)|v|_{\max} + Y_{v|v|}|v^2|_{\max} + |w_2|_{\max}\right)$.

Based on Young's inequality, the first three uncertainty terms in Eq. (43) are less than the following functions for positive constants ς_i (i = 1, 2, 3): $\frac{1}{2}k_y |r|_{\max}\left(\varsigma_1 v_e^2 + \varsigma_1^{-1} x_e^2\right)$, $\frac{1}{2}\left(|\dot{v}_Q|_{\max} + |k_y v_Q|_{\max} + |k_\psi m_v^{-1} m_u u|_{\max}\right)\left(\varsigma_2 v_e^2 + \varsigma_2^{-1}\psi_e^2\right)$ and $\frac{1}{2}\left(\varsigma_3 v_e^2 + \varsigma_3^{-1} y_e^2\right)$. Let us examine the last three uncertainties terms in Eq. (43) using a worst case analysis by assuming all of them are positive. In this case, Eq. (43) becomes

$$\dot{V}_5 \le -\lambda_x x_e^2 - \lambda_y y_e^2 - \lambda_u u_e^2 - \lambda_\psi \psi_e^2 - \lambda_r r_e^2 - \lambda_v v_e^2 + \zeta |v_e| \quad (44)$$

where

$$\lambda_x = k_x - 0.5\varsigma_1^{-1} k_y |r|_{\max};\ \lambda_y = k_y - 0.5\varsigma_3^{-1};\ \lambda_u = k_u\text{'}\ \lambda_r = k_r;$$

$$\lambda_\psi = k_\psi - 0.5\varsigma_2^{-1}\left(|\dot{v}_Q|_{\max} + |k_\psi v_Q|_{\max} + |k_\psi m_v^{-1} m_u u|_{\max}\right) \text{ and}$$

$$\lambda_v = -0.5 k_\psi |r|_{\max}\varsigma_1 - 0.5\varsigma_3 - 0.5\varsigma_2\left(|\dot{v}_Q|_{\max} + |k_y v_Q|_{\max} + |k_\psi m_v^{-1} m_u u|_{\max}\right).$$

Under various different conditions, the appropriate values of k_x, k_y, k_u, k_ψ, ς_1, ς_1 and ς_3 can be selected to ensure a positive value for λ_x, λ_y and λ_u. By taking $x(t) = [x_e, y_e, \psi_e, u_e, v_e, r_e]^T$ and γ = min $\{\lambda_x, \lambda_y, \lambda_u, \lambda_\psi, \lambda_r, \lambda_v\}$, inequality (44) becomes $\dot{V}_5 \le -2\gamma V_5 + \zeta |v_e|$, which results in $V_5(t) \le V_5(0)e^{-2\gamma t} + 0.5\zeta |v_e| \gamma^{-1}$ for $t \in \left[0, t_{final}\right)$ using the Comparison Lemma (Khalil, 1996). Thus, the following conclusion can be drawn:

$$\|x(t)\| \le \|x(0)\| e^{-\gamma t} + \sqrt{\zeta |v_e| \gamma^{-1}},\ t \in \left[0, t_{final}\right) \quad (45)$$

Eq. (45) indicates that the state errors remain in a bounded setting near zero and can be reduced by increasing the gains in Eq. (44). Since $u_r = k_x x_e + v_Q \cos\psi_e$, $v_r = k_y y_e + v_Q \sin\psi_e$, and $r_r = \dot{\psi}_R + k_\psi \psi_e$, the velocity tracking errors of u_e, v_e and r_e can also be kept in a bounded setting near zero when the state errors of $\|x(t)\|$ converge to a value with a small neighborhood near zero, which would ensure the global stability of the control system.

VI. NUMERAL SIMULATION RESULTS AND DISCUSSIONS

Numerical simulations were conducted to evaluate the proposed controller performances in model's smooth transient responses, quick convergence, low control effort, and robustness. To verify the validity of the proposed controller, an underactuated underwater vehicle was taken as an example to evaluate its ability in the trajectory tracking control. For the vehicle considered in this example, the following vectors are used $\upsilon = [u, v, r]^T$, $\eta = [x, y, \Psi]^T$ and $\tau = [F_u, 0, \tau_r]^T$. In the following simulations, the same controller structure is applied for the surge force of F_u and the yaw torque of τ_r using the same gain values in the controller equations. In that way, the controller design would be independent of the tracked trajectory. The mass (m) of the underactuated underwater vehicle is 185 kg and its rotational inertia around z axis (I_z) *is* 50 kg·m^2. The added masses in the directions of u and v and the added moment of inertia in the direction of r are given as $X_{\dot{u}} = -30$ kg, $Y_{\dot{v}} = -80$ kg and $N_{\dot{r}} = -30$ kg·m^2, respectively. The surge, sway and yaw linear drag coefficients have values of X_u = 70 kg/s, Y_v = 100 kg/s and N_r = 50 kg·m^2/s. The surge, sway, and yaw quadratic drag coefficients are at $X_{u|u|}$ = 100 kg/m, $Y_{v|v|}$ = 200 kg/m and $N_{r|r|}$ = 100 kg·m^2. Also, the constants of m_u, m_v, m_r representing the added mass and combined inertia are given as $m_u = m - X_{\dot{u}} = 215$ kg, $m_v = m - Y_{\dot{v}} =$ 265 kg, and $m_r = I_z - N_{\dot{r}} = 80$ kg·m^2.

All values mentioned above were used as the nominal values in the controller's dynamic model. In the following simulation cases, the model parameters in the plant's dynamic model including physical parameters of the underwater vehicle and hydrodynamic coefficients are determined based on the following two assumptions:

(1) the actual values are not known;
(2) the actual values vary within ±10% from the nominal values.

For example, the nominal values of the five parameters in the controller's dynamic model $\left\{\hat{m}, \hat{I}_z, \hat{X}_{\dot{u}}, \hat{X}_{|u|u}\right\}$ are equal to {185 kg, 50 kg·m^2, -30 kg, 100 kg/m} and their corresponding actual values in the plant's dynamic model can be selected within the following ranges: $m \in$ [166.5 kg, 203.5 kg], $I_z \in$ [49.5 kg·m^2, 50.5 kg·m^2], $X_{\dot{u}} \in$ [-30.3 kg, -29.7 kg], $X_{|u|u} \in$ [90 kg/m, 110 kg/m]. Numerical simulations were carried out using the fourth-order Runge-Kutta formula with a constant time step at 0.002 s. The initial conditions and control parameters were given as follows: k_x = 15, k_y = 65, k_u =2, $k_\psi = k_r$ = 1.5, ρ_1 = 40, ρ_3 = 8, $\sigma_1 = \sigma_2$ = 0.8.

Three adaptive fuzzy terms in the form of Eq. (18) were used to approximate the three uncertainties of $\Theta_1 = -X_u^* u - X_{u|u|}^* u|u|$, $\Theta_2 = -Y_v^* v - Y_{v|v|}^* v|v|$, and $\Theta_3 = -N_r^* r - N_{r|r|}^* r|r|$ in

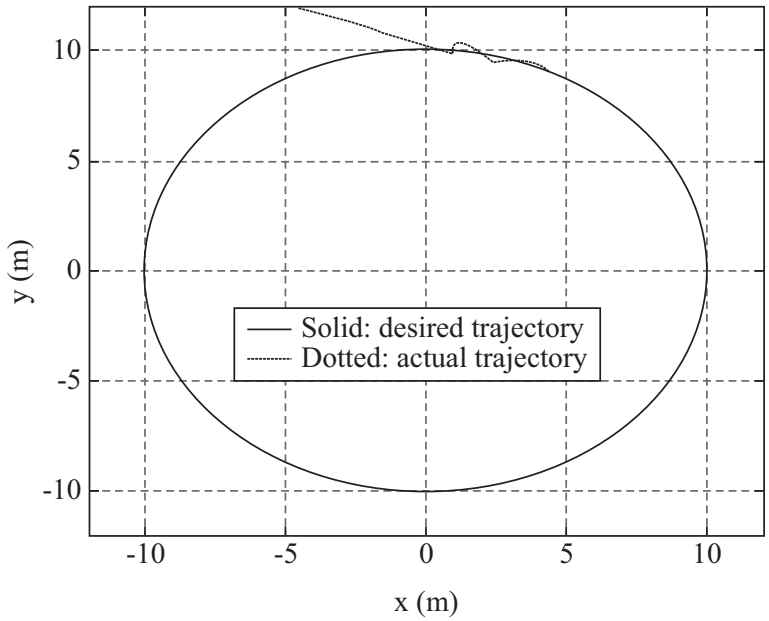

Fig. 3. Circular tracking control comparison between the actual and desired trajectories using nominal model parameters.

Eq. (2). The input vector of the three adaptive fuzzy terms is defined as $e_s = [u_e, v_e, r_e]^T$. According to the errors caused by uncertainties, the universe of discourse of each fuzzy input vector is divided into five fuzzy labels and their corresponding membership functions are defined as $u_{A_i}(e_{si}) = \exp\left[-(e_{si} - c_i)^2 / 2\sigma_i^2\right]$, where c_i has the values of -1, -0.5, 0, 0.5 and 1 and σ_1 is equal to 0.2124. The fuzzy basis function $\varphi(e_s)$ in Eq. (18) was selected as $\varphi(e_s) = [\varphi_1(e_s), \ldots, \varphi_M(e_s)]$, where the *l-th* fuzzy basis function was designed as $\varphi_l(e_s) = \prod_{i=1}^{12} \mu_{A_i^l}(e_{si}) \Big/ \sum_{l=1}^{M} \prod_{i=1}^{12} \mu_{A_i^l}(e_{si})$ with $\mu_{A_i^l}(e_{si})$ as the membership function of the *i-th* input vector in the *l-th* fuzzy rule and M as the number of rules. Based on the above approximations, we have $\hat{\Theta}_i = -\hat{\eta}_i^T \varphi(e_s) \tanh\left(\dfrac{\hat{\eta}_i^T \varphi(e_s)}{\varepsilon}\right)$. The constant of λ_1 in the parameter adaptive law (19) was selected as $\lambda_1 = 100$.

To evaluate the trajectory tracking control performances of the proposed controller, two different responses were obtained under the following two conditions:

(a) The actual model parameters are known and
(b) The actual model parameters have values within ±10% of its corresponding nominal values.

The proposed controller was forced to track a desired circular path of $x_R(t) = 10 \sin(0.01t)$ m, $y_R(t) = 10 \cos(0.01t)$ m. In this case the second derivatives of the path are required since the circular tracking of the vehicle is achieved by a constant angular velocity of r_R and linear velocities of u_R and v_R. It is found that $v_Q = 0.1$ m/s and $\dot{v}_Q = 0$ from Eq. (6) and $\omega = -0.01$ rad / s from Eq. (7), which indicates that the vehicle travels along a constant clockwise path.

Case 1:

The case focuses on the trajectory tracking control for a circular path based on the nominal model parameter. In this case, the underactuated underwater vehicle moves from the initial position $\eta = [-5 \text{ m}, 15 \text{ m}, 0 \text{ rad}]^T$ at an initial velocity of $v = [0.01$ m/s, 0 m/s, 0 rad/s$]^T$, which has initial position and orientation errors at $|x_e| = 5$ m, $|y_e| = -2$ m and $|\psi_e| = 0°$ and initial velocity errors at $|u_e| = 0.09$ m/s, $|v_e| = 0$ m/s and $|r_e| = -0.01$ rad/s. The total simulation time was set as 640 s. For the purpose of better observation of the transient and steady state responses, the trajectory tracking errors were displayed for the first 100 seconds and for the entire duration of 640 seconds. The trajectory of the underactuated underwater vehicle is displayed in the inertial frame plane, as shown in Fig. 3. The solid line is the desired path while the dashed line represents the actual path calculated by the proposed controller. It can be seen from Fig. 3 that a large difference exists between the desired path and the simulation datum during the transient state response.

The surge control force of F_u and the yaw control moment of τ_r are illustrated in Fig. 4. It is observed from Fig. 4 that the surge control force of F_u and yaw control moment of τ_r are very high at the initial 20 s and gradually converge to their desired values after a short of period of time. During the steady state response after the convergence, both the surge force and the yaw moment exhibit a favorable steady performance without any significant big overshoot.

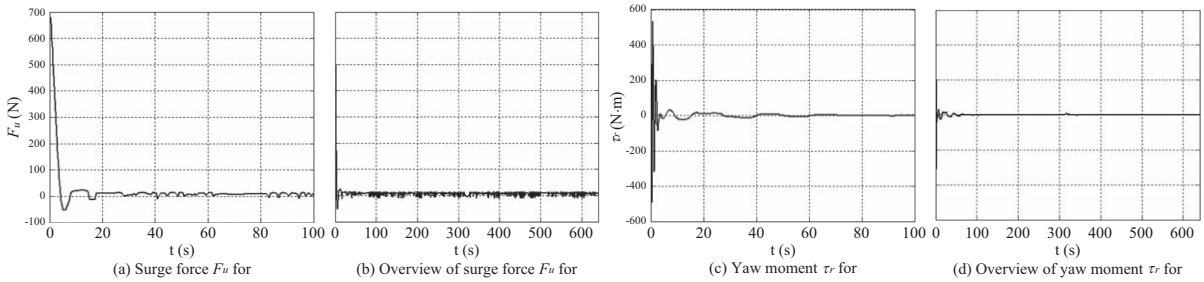

(a) Surge force F_u for the first 100 seconds (b) Overview of surge force F_u for the entire duration (c) Yaw moment τ_r for the first 100 seconds (d) Overview of yaw moment τ_r for the entire duration

Fig. 4. Responses of the surge control force and the yaw control moment.

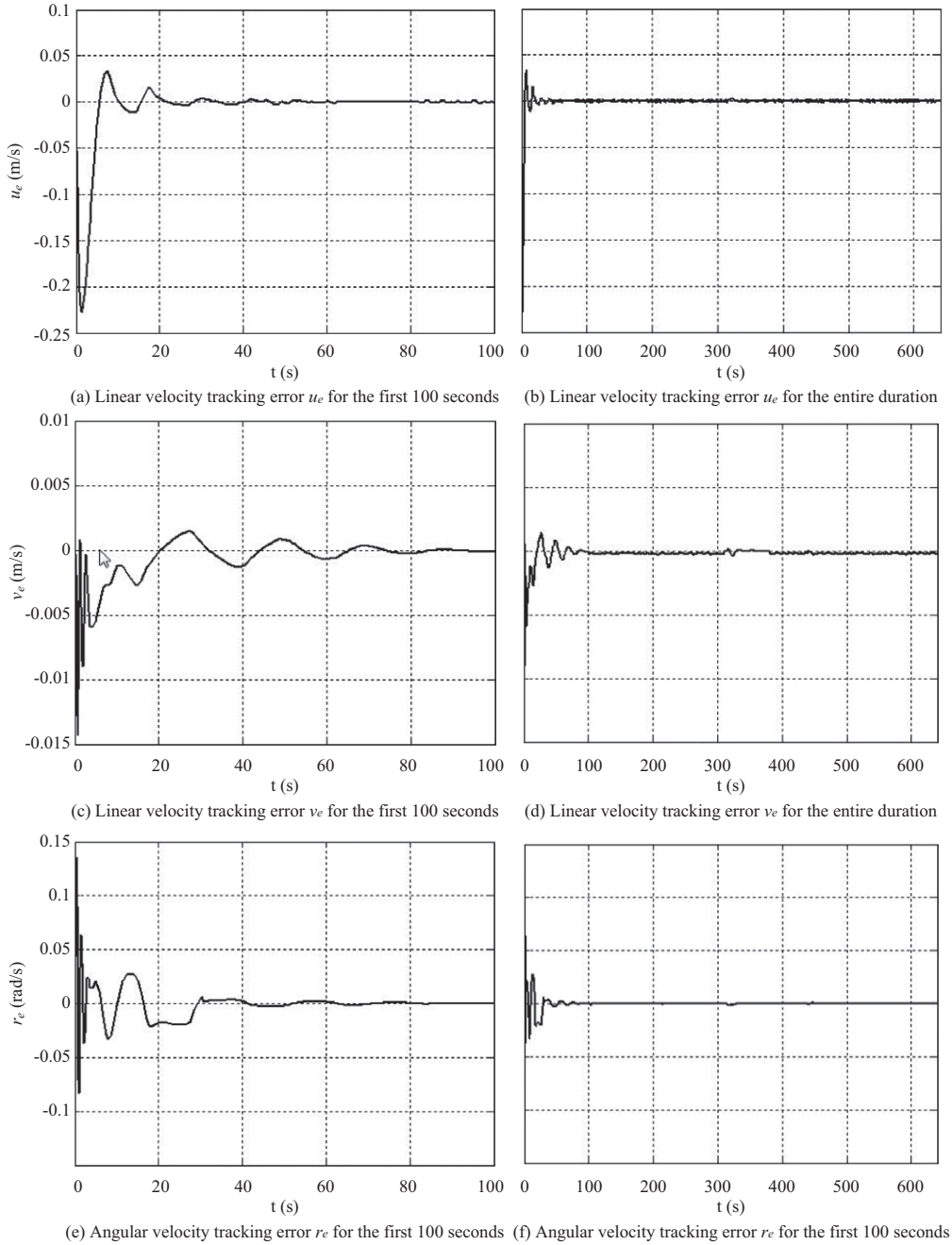

(a) Linear velocity tracking error u_e for the first 100 seconds (b) Linear velocity tracking error u_e for the entire duration

(c) Linear velocity tracking error v_e for the first 100 seconds (d) Linear velocity tracking error v_e for the entire duration

(e) Angular velocity tracking error r_e for the first 100 seconds (f) Angular velocity tracking error r_e for the first 100 seconds

Fig. 5. Velocity tracking errors in the body-fixed frame.

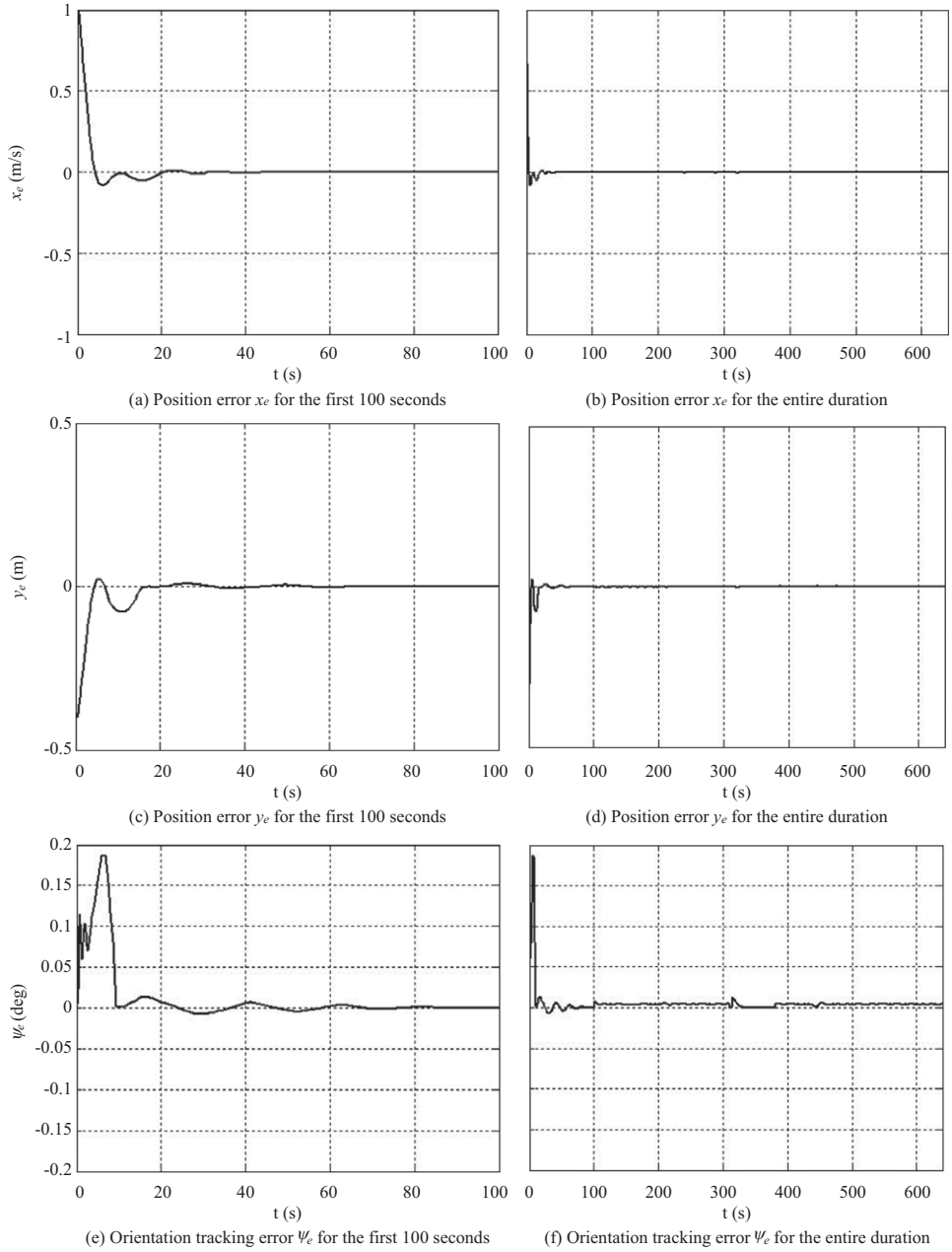

Fig. 6. Position and orientation tracking errors in the inertial frame.

The velocity tracking errors in the body-fixed frame are shown in Fig. 5, in which the left figures display the errors for the first 100 s of the simulation time to observe the transient response and the right figures display the errors for the entire duration of 640 s to provide an overall view of the errors. It can be seen from Fig. 5 that the velocity tracking errors converge to a value near zero with an oscillation the order of 10^{-3} m/s or rad/s without any large overshoot and then slowly converge to a steady response toward zero after 30 s. Once the velocity tracking errors reach the steady state, the variation in errors is very limited. The maximum absolute velocity errors of u_e, v_e, r_e calculated from the data shown in Fig. 5 are 0.0035 (m/s), 0.0013 (m/s), 0.0061 (rad/s), respectively and their corresponding standard deviations are 0.98367×10^{-3} (m/s), 0.16537×10^{-3} (m/s) and 0.62076×10^{-3} (rad/s).

The position and orientation tracking errors are depicted in Fig. 6, in which the left figures shows data for the first 100 s simulation time and the right figures shows the data for the entire simulation duration of 640 s. It is observed from the left figures that after a short period of time, the tracking errors converge to near zero with a small oscillation in the order of 10^{-3} m or deg. The position tracking errors of x_e and y_e calculated from the data in Fig. 6 are within the range from -0.0083 m to 0.0046 m and the orientation tracking error varies within the range from

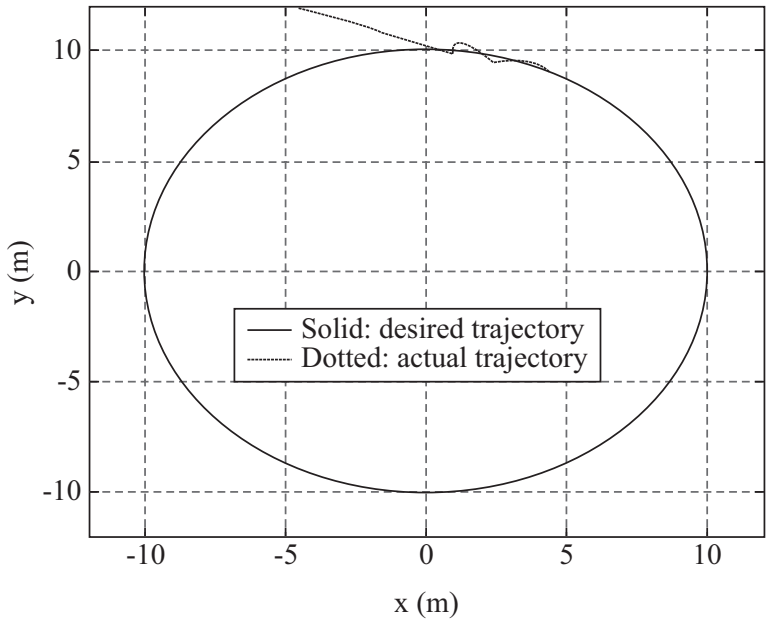

Fig. 7. Circular trajectory comparison between the desired path and actual path using the model parameters within ±10% of the nominal values.

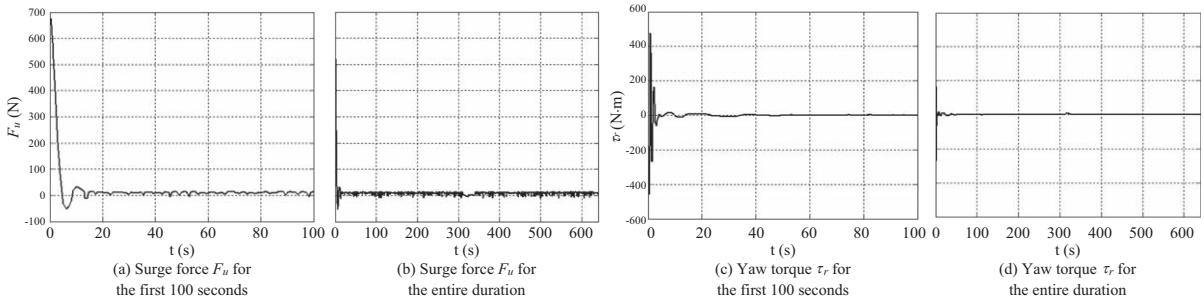

Fig. 8. The surge control force and yaw control torque using the model parameters within ±10% of the nominal values.

-0.0072 rad to 0.0126 rad. The results demonstrate that the proposed controller performs extremely well in trajectory tracking control and quick convergence.

Case 2:

In this case, it is assumed that the actual model parameters are not known but they are within a maximal uncertainty of ±10% of the nominal values for the previous trajectory tracking control around a circular path. The initial conditions are the same as those in Case 1. The trajectory of the underactuated underwater vehicle in the inertial frame is displayed in Fig. 7. It can be observed from Fig. 7 that similar errors exist between the desired path and the simulation datum. When compared to the results from Case 1, the proposed controller in this case can also effectively eliminate uncertainties although it has the unknown model parameters.

Fig. 8 demonstrates the surge control force of F_u and the yaw control torque of τ_r resulted from the proposed controller. It is noteworthy that the estimated control force and torque exhibit relatively small oscillations even though the unknown model parameters are assumed.

The velocity tracking errors in the body-fixed frame are displayed in Fig. 9, in which the left figures display the results for the first 100 s of the simulation time and the right figures illustrate the results for the entire duration of 640 s. The velocity tracking errors quickly converge to a near zero value with a very small oscillation in the order of 10^{-3} m/s or rad/s and reach to the steady state after a short period of time. Once the velocity tracking errors reach to the steady state, the oscillation range is evenly bounded with the maximum absolute velocity errors of u_e, v_e, r_e at 0.0033 (m/s), 0.00054583 (m/s), 0.0074 (rad/s), respectively and the corresponding standard deviations at 0.00096979 (m/s), 0.000095202 (m/s) and 0.00046292 (rad/s). When compared to the results from Case 1, the unknown dynamic model parameters in this case resulted in the similar velocity tracking errors to those from Case 1. Those results confirm that the proposed controller is effective in uncertainty elimination.

The position and orientation tracking errors are depicted in

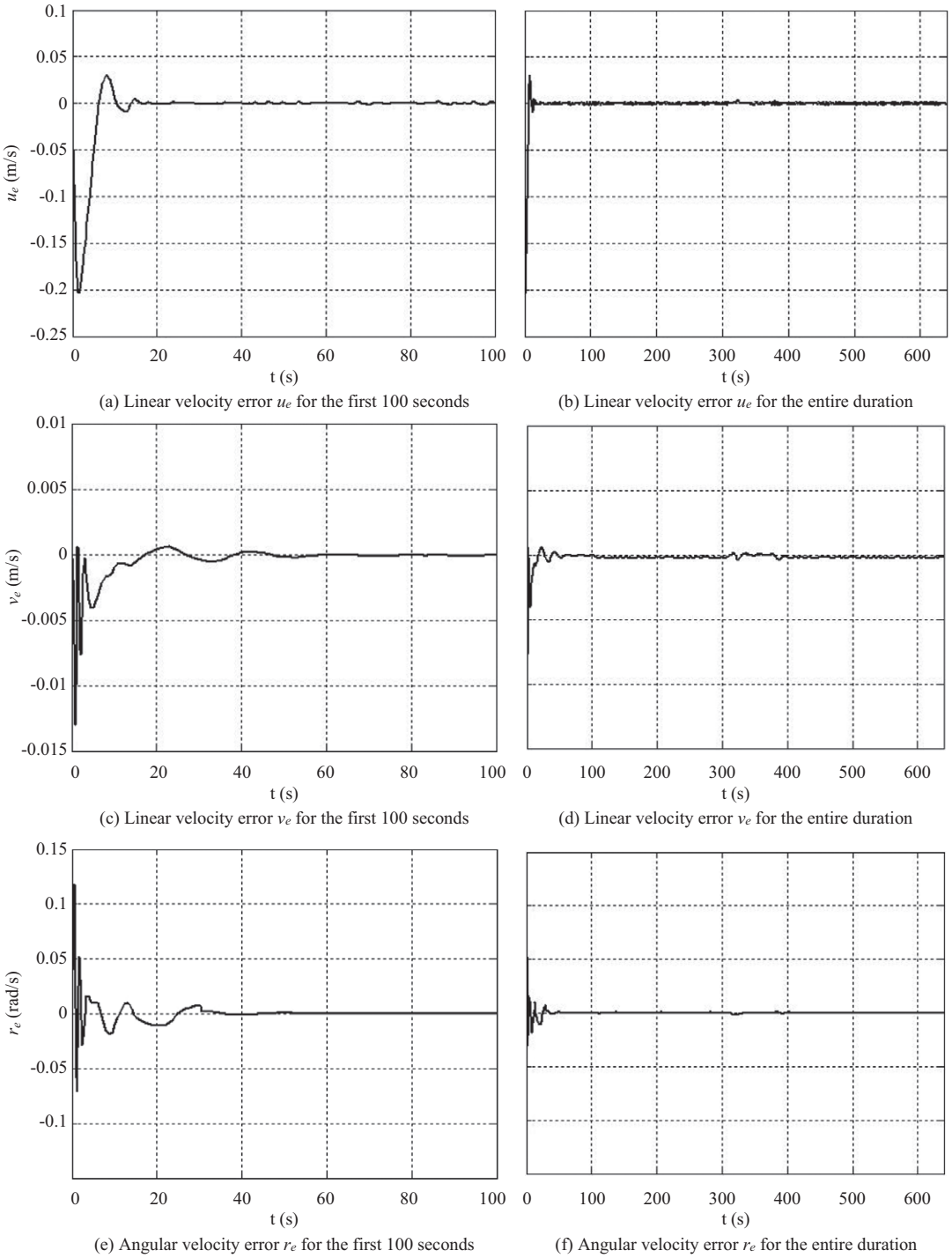

Fig. 9. Velocity tracking errors in the body-fixed frame using the model parameters within ±10% of the nominal values.

Fig. 10. They both quickly converge to a near zero value and stabilize at this value with an oscillation in the order of 10^{-3} m or deg. The position tracking errors of x_e and y_e vary within the range from -0.0055 m to 0.004 m the orientation tracking error varies from -0.0045 rad to 0.0126 rad. The results show that although some unknown model parameters are assumed in the second case, the proposed controller performs extremely well and also shows its capability of converging quickly.

VII. CONCLUSIONS

In this paper, the composite robust control scheme coupled with the sliding mode controller and the adaptive fuzzy control algorithm was introduced to tackle the horizontal trajectory

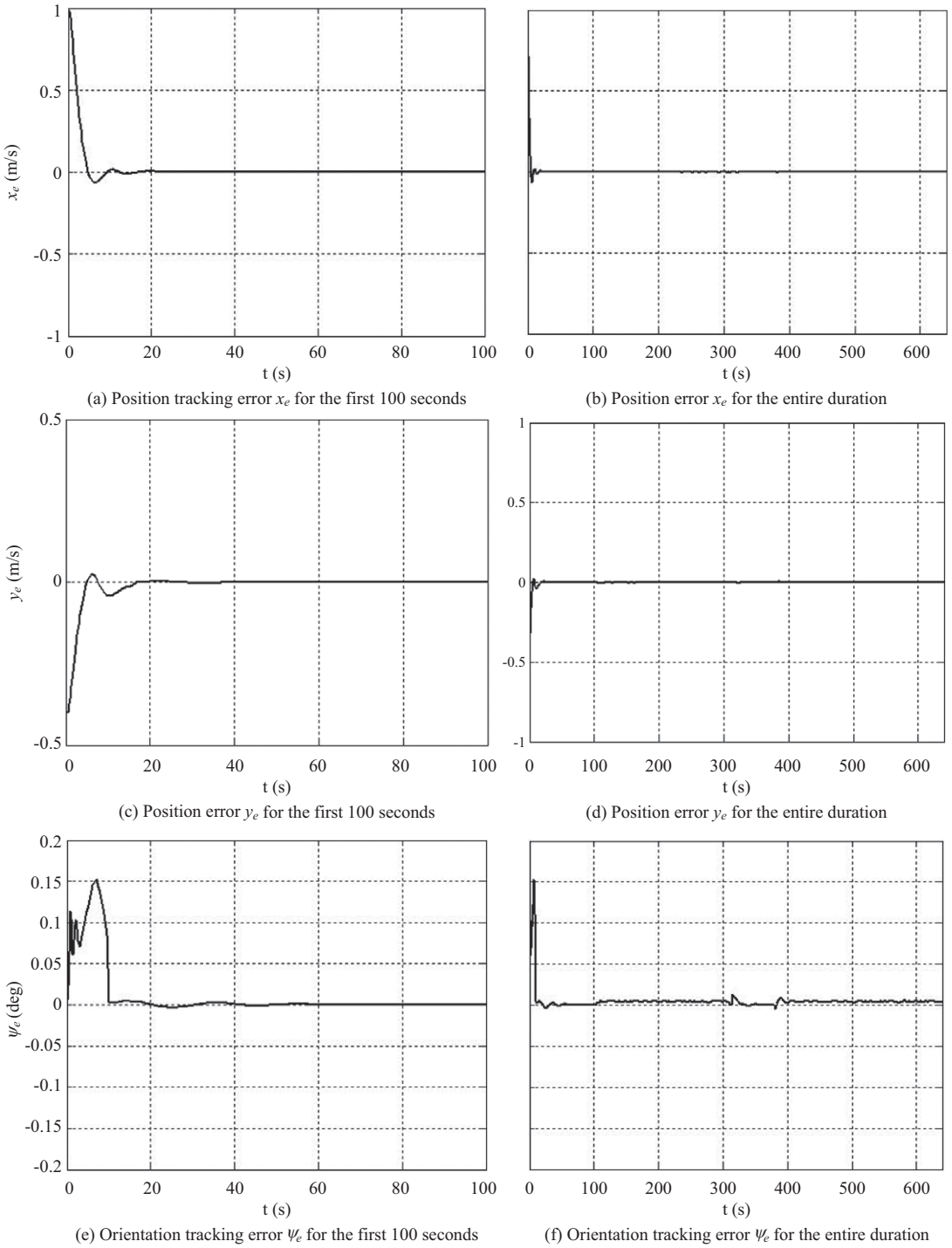

Fig. 10. Position tracking errors in the inertial frame using the control parameters within ±10% of the nominal values.

tracking control problem for underactuated underwater vehicles with model parameter perturbations and environmental disturbances. An adaptive fuzzy control algorithm was employed to compensate for model parameter perturbations while a sliding mode controller was adopted to eliminate the effects of environmental disturbances and approximation errors. The asymptotic stability of the overall system was demonstrated based on Lyapunov stability theory. The relation between sliding mode control gains and model parameter uncertainties was derived to determine the error eliminating ability of the controller. The horizontal dynamic model and tracking error equations for the underactuated underwater vehicle were established for the trajectory tracking control of the vehicle.

The proposed control scheme was also simulated for a circular

path using the nominal and non-nominal parameters and its efficiency in eliminating the uncertainties was demonstrated and validated using numerical simulations of a 3-DOF underactuated underwater vehicle. Numerical simulation results demonstrated that the proposed controller displayed excellent performances in its smooth transient responses, quick convergence, low control effort, and robustness. The proposed controller can be used to analyse the control performances of the controller under various operational conditions.

ACKNOWLEDGEMENTS

Grateful acknowledgement is given to the financial supports from the National Natural Science Foundation of China with Grant No. 51375264 and Science and Technology Major Project of Shandong Province with Grant No. 2015JMRH0218. This work was also partially supported by State Key Laboratory of Robotics and System (HIT) with Grant No. SKLRS-2015-MS-06, and China Post-doctoral Science Foundation with Grant No. 2014T70632 and 2013M530318, and Research Awards Fund for Excellent Young and Middle-aged Scientists of Shandong Province with Grant No. BS2013ZZ008.

REFERENCES

Atrp, S., Z. Q. Leong, D. Ranmuthugala, A. L. Forrest and J. Duffy (2015). Numerical investigation of the hydrodynamic interaction between two underwater bodies in relative motion. Applied Ocean Research 51, 14-24.

Brockett, R. W. (1983). Asymptotic stability and feedback stabilization. Differential Geometric Control Theory 181-191.

Chen Y., R. M. Zhang, X. Y. Zhao and J. Gao(2016). Adaptive fuzzy inverse trajectory tracking control of underactuated underwater vehicle with uncertainties. Ocean Engineering 121, 123-133.

Geranmehr, B. and S. R. Nekoo (2015). Nonlinear suboptimal control of fully coupled non-affine six-DOF autonomous underwater vehicle using the state-dependent Riccati equation. Ocean Engineering 96, 248-257.

Ghommam, J. and M. Saad (2013). Backstepping-based cooperative and adaptive tracking control design for a group of underactuated AUVs in horizontal plan. International Journal of Control 87, 1076-1093.

Jia, H. M., W. L. Song and Z. L. Chen (2012). Nonlinear backstepping control of underactuated AUV in diving plane. Advances in information Sciences and Service Sciences 4, 214-221.

Khalid, I., M. R. Arshad and I. Syafizal (2014). A hybrid-driven underwater glider model, hydrodynamics estimation, and an analysis of the motion control. Ocean Engineering 81, 111-129.

Khalil, H. (1996). Nonlinear Systems. Prentice-Hall, Englewood Cliffs.

Khodayari, M. and S. Balochian (2015). Modeling and control of autonomous underwater vehicle (AUV) in heading and depth attitude via self-adaptive fuzzy PID controller. Journal of Marine Science and Technology 20, 559-578.

Koh, T. H., M. W. S. Lau, G. Seet and E. Low (2006). A control module scheme for an underactuated underwater robotic vehicle. Joumal of Intelligent and Robots Systems 46, 43-58.

Li, Y., C. Wei, Q. Wu, P. Y. Chen, Y. Q. Jiang and Y. M. Li (2015). Study of 3 dimension trajectory tracking of underactuated autonomous underwater vehicle. Ocean Engineering 105, 270-274.

Park, B. S. (2014). Neural network-based tracking control of underactuated autonomous underwater vehicles with model uncertainties. Journal of Dynamic Systems Measurement & Control 137, 1-7.

Polycarpou, M. M. and P. A. Ioannou (1996). A robust adaptive nonlinear control design. Automatica 32, 423-427.

Qi, X. (2015). Spatial target path following control based on Nussbaum gain method for underactuated underwater vehicle. Ocean Engineering 104, 680-685.

Raimondi, F. M. and M. Melluso (2010). Fuzzy/kalman hierarchical horizontal motion control of underactuated ROVs. International Journal of Advanced Robotic Systems 7, 139-154.

Thor, I. and T. I. Fossen (2002). Marine Control Systems: Guidance, Navigation and Control of ships, Rigs and Underwater Vehicles. Trondheim, Norway.

Xu, J., M. Wang and L. Qiao (2015). Dynamical sliding mode control for the trajectory tracking of underactuated unmanned underwater vehicles. Ocean Engineering 105, 54-63.

Yan, Z. P., H. M. Yu, W. Zhang, B. Y. Li and J. J. Zhou (2015). Globally finite-time stable tracking control of underactuated UUVs. Ocean Engineering 107, 132-146.